Concomitant activation of Cl^- and K^+ currents by secretory stimulation in human epithelial cells

Isabelle Baró, Brigitte Roch, Anne-Sophie Hongre and Denis Escande*

Laboratoire de Physiologie Cellulaire, URA CNRS 1121, Bât 443, Université Paris XI, 91405 Orsay, France

1. Whole-cell currents were investigated in the model salt-secreting epithelium, human T84 cell line, by means of the perforated patch-clamp technique. In the control extracellular medium containing Cl^-, depolarizing voltage ramps evoked current responses which peaked at $5{\cdot}43 \pm 0{\cdot}81$ pA pF^{-1} at +60 mV and had a reversal potential (E_{rev}) of $-38{\cdot}4 \pm 2{\cdot}5$ mV ($n = 23$).

2. Activation of the cAMP pathway with forskolin increased the current at +60 mV from $3{\cdot}81 \pm 0{\cdot}61$ to $20{\cdot}79 \pm 5{\cdot}08$ pA pF^{-1} ($n = 18$). In thirteen cells, E_{rev} was initially shifted towards positive potentials (E_{rev} of the cAMP-activated initial current was $-18{\cdot}2 \pm 1{\cdot}2$ mV) and subsequently shifted towards more negative potentials, consistent with the activation of both Cl^- and K^+ currents during cAMP stimulation.

3. Increasing the intracellular Ca^{2+} concentration, $[Ca^{2+}]_i$, with ionomycin (1 μM) or with acetylcholine (1 μM), increased the current at +60 mV from $7{\cdot}79 \pm 1{\cdot}57$ to $57{\cdot}50 \pm 12{\cdot}10$ pA pF^{-1} ($n = 6$) and from 6·36 to 34·13 pA pF^{-1} ($n = 4$), respectively. With both agonists, E_{rev} was shifted either towards the reversal potential for potassium, E_K, or towards the reversal potential for chloride, E_{Cl}, depending on the cell.

4. In the absence of chloride ions (gluconate substituted), stimulation of the Ca^{2+} pathway activated a time-independent outward current of large amplitude. This current exhibited inward rectification at positive voltages, reverted at $-89{\cdot}5 \pm 0{\cdot}2$ mV and was markedly reduced by charybdotoxin (10 nM), a specific blocker of Ca^{2+}-activated K^+ channels. When a voltage step protocol was used, increased $[Ca^{2+}]_i$ also activated an outward current at potentials more positive than −40 mV which slowly relaxed during depolarizing steps.

5. The activation of both (i) a time-independent inwardly rectifying charybdotoxin-sensitive K^+ current, and (ii) a time-dependent slowly inactivating current was also produced by cAMP stimulation.

6. We concluded that (i) in the T84 epithelial cells, both Cl^- and K^+ currents are concomitantly increased by secretagogue stimulation, and (ii) two different types of K^+ conductances are activated by either the cAMP or the intracellular Ca^{2+} secreting pathways.

The transepithelial transport of Cl^- is central to fluid secretion across many epithelia including those of the airways and of the intestine (Quinton, 1990; Halm & Frizzell, 1990; McCann & Welsh, 1990). The stimulatory effects of receptor-mediated agonists on Cl^--secreting epithelia are transduced by cAMP and Ca^{2+}-dependent regulatory pathways (McRoberts, Beuerlein & Dharmsathaphorn, 1985; Weymer, Huott, Liu, McRoberts & Dharmsathaphorn, 1985; Dharmsathaphorn & Pandol, 1986; Mandel, Dharmsathaphorn & McRoberts, 1986*a*; Wasserman, Barrett, Huott, Beuerlein, Kagnoff & Dharmsathaphorn, 1988; Dharmsathaphorn, Cohn & Beuerlein, 1989). The consensus view for active Cl^- transport across secreting epithelia involves: (i) a bumetamide-sensitive Cl^- pathway located at the basolateral membrane, and (ii) various Cl^--channel proteins situated at the apical surface (Worrell, Butt, Cliff & Frizzell, 1989; Tabcharani, Low, Elie & Hanrahan, 1990; Anderson & Welsh, 1991; Worell & Frizzell, 1991; Wagner, Cozens, Shulman, Gruenert, Stryer & Garner, 1991; Chan,

*To whom reprint requests should be addressed.

Kaetzel, Nelson, Hazarika & Dedman, 1992; Halm & Frizzell, 1992; Lin, Nairn & Guggino, 1992). According to this model, Cl^- preferentially penetrates the cells basolaterally, together with Na^+ and K^+, through a Na^+–K^+–$2Cl^-$ cotransporter. Na^+ ions accompanying Cl^- ions are pumped out through the basolateral Na^+–K^+-ATPase. Thus a basolateral inward flow of K^+ is the consequence of Cl^- entry through the Na^+–K^+–$2Cl^-$ cotransporter but also of Na^+ extrusion through the Na^+–K^+-ATPase pump. To prevent changes in the cell volume, these K^+ charges are necessarily extruded back via basolateral K^+ conductances. Furthermore, Cl^- ions are secreted through apical Cl^- channels down a favourable electrical gradient but against an unfavourable chemical gradient. If stimulation by secretory agonists were to result only in the activation of apical Cl^- channels, then the membrane potential would instantaneously shift towards the equilibrium potential for Cl^- ions, and the Cl^- efflux would stop. It has been shown that Cl^- secretion may increase eight- to ninefold on stimulation (Shorofsky, Field & Fozzard, 1984). Therefore, a comparable increase in the activity of K^+ channels is required: (i) to recycle K^+ ions and (ii) to maintain the apical membrane at a more negative potential than the Cl^- equilibrium potential.

In the present study, we used the perforated patch-clamp technique in human T84 cells to demonstrate directly coupled activation of both Cl^- and K^+ conductances by secretagogues.

METHODS

Cell culture

The T84 cell line is a human colonic carcinoma cell line that was obtained from a lung metastase in a patient. The cells used in the present work were provided by the American Type Culture Collection (CCL 248; ATCC, Rockville, MD, USA). They were cultured in a 1:1 mixture of Dulbecco's modified Eagle's medium and Ham's F-12 medium supplemented with L-glutamine, 15 mM Hepes, 5% (v/v) fetal calf serum and 1% antibiotics (penicillin 10000 i.u. ml^{-1}; streptomycin 10000 g ml^{-1}; all obtained from Gibco, Paisley, Strathclyde, UK), at 37 °C in a humidified 5% CO_2–95% air incubator, and regularly subcultured by enzymatic treatment with a solution of 0·25% trypsin, 1 mg ml^{-1} EDTA in a Ca^{2+}- and Mg^{2+}-free phosphate buffer solution (Gibco). Cells from passage 56 to 70 were used 1–3 days after plating on coated plastic Petri dishes (Nunclon; InterMed Nunc, Roskilde, Denmark). Individual cells or, occasionally couples or tetrads were studied only, in order to limit voltage-clamp artifacts arising from cell-to-cell coupling.

Solutions

The standard Tyrode solution used for patch-clamp experiments contained (mM): NaCl, 145; KCl, 4; $MgCl_2$, 1; $CaCl_2$, 1; Hepes, 5; glucose, 5; pH adjusted to 7·4 with NaOH. In addition, 60 mM mannitol was added to the locally perfused external solution. The pipette solution contained (mM): KCl, 74·5; potassium aspartate, 70·5; Hepes, 5; pH adjusted to 7·2 with KOH. Nystatin (Sigma Chemical Co., St Louis, MO, USA) kept for a short time in stock solution (40 mg ml^{-1} in dimethyl sulphoxide) was added to the pipette solution (final concentration, 350 μg ml^{-1}). This pipette solution was used for 1–2 h before replacement.

In experiments specifically aimed to record K^+ currents, Cl^--free solutions were used. Cl^- and aspartate were omitted from the standard extracellular and pipette solutions and replaced by an equimolar amount of gluconate, an anion that is almost impermeable through T84 Cl^- channels (Halm & Frizzell, 1992). Under these conditions, the external free Ca^{2+} and Mg^{2+} concentrations were calculated at 0·29 and 0·57 mM, respectively.

Patch-clamp experiments

A Petri dish containing cells was placed on the stage of an inverted microscope (CK2; Olympus Optical Co. Ltd, Tokyo) into a torus-shaped water jacket (home made) heated at 35 °C (polystat 86602; Bioblock Scientific, Illkirch, France). The cells were continuously superfused with the standard solution at 35 °C. The 'perforated patch' configuration described by Horn & Marty (1988) was used to record whole-cell currents. In this configuration, the membrane patch was permeabilized with nystatin instead of being ruptured after the gigohm-seal formation, in order to preserve the integrity of the intracellular medium. Nystatin forms pores in the membrane patch which are permeable to small monovalent cations, but which do not penetrate into the cytoplasm. Typically, the serial resistance decreased to a steady state below 20 MΩ after 5–15 min of nystatin action, thus allowing whole-cell currents to be accurately recorded. It must be noted that, under these circumstances, a constant error of a few millivolts is made in holding and measurement of the cell potential, and that the cell is hyperosmotic to the pipette and external solutions (Horn & Marty, 1988). To prevent changes in cell volume, mannitol was added to the locally perfused medium. Data reported in the present article are expressed as measured values, i.e. the potential was not corrected. It is understood that a shift in the I–V curve may have occurred, but since comparisons between currents were made under the same experimental conditions, this purported shift did not interfere with the observed effects.

Patch pipettes were pulled in two stages from soda-lime glass capillary tubes (73811; Kimble, Toledo, OH, USA) using a pipette puller (L/M-3P-A; List Medical, Darmstadt, Germany). Pipette tip resistance measured in control solution ranged between 2·5 and 5 MΩ when filled with the pipette solution. The pipette was electrically connected to a patch-clamp amplifier (Axopatch 200A; Axon Instruments Inc., Foster City, CA, USA). A reference electrode made from Ag–AgCl wire was connected to the bath through an agar bridge saturated with 145 mM KCl solution. On one side of the vertical bench (PCS 1000; Biologic, Claix, France) surrounding the microscope, a Narashige three-axis micromanipulator (MO-103; Narashige Scientific Instrument Lab, Tokyo, Japan) mounted on a manipulator (MM33; Biologic) was used to hold the headstage (CV 201A; Axon Instruments Inc.) and to approach the cell with the pipette. On the other side, a microperfusion system composed of joined Tygon capillaries (i.d. 0·25 mm), mounted on a one-axis micromanipulator (MO-22; Narashige) and on a manipulator (MM33; Biologic) allowed local application and rapid change of different experimental solutions. The solutions were perfused by gravity and the bath volume was maintained with a pump (Medcalf Bros Ltd, Herts, UK). A 486/33 personal computer coupled with an A/D

converter (Tecmar TM100 Labmaster; Scientific Solution, Solon, OH, USA) acted as a stimulator and data recorder. Stimulation, data recording and analysis were performed using software developed in the laboratory by Gérard Sadoc. Voltage steps 2 mV in amplitude were imposed via the pipette and the seal resistance was calculated. When a gigohm seal between the patch pipette and the cell membrane was obtained, the holding potential was clamped to −60 mV, and 10 mV voltage steps were then imposed. The membrane resistance (R_m), the serial resistance (R_s) and the membrane capacitance (C_m) were also monitored. Only cells in which R_s reached values below 20 MΩ were retained for further recording. A value of mean C_m (33·6 ± 1·5 pF, $n = 70$) was calculated in the Cl^--containing medium for the cells used in these experiments. The resting membrane potential was kept at −60 mV and voltage ramps from −80 to +60 mV were imposed (70 mV s^{-1}, 0·2 Hz). This stimulation protocol provides direct records of the current–voltage relationship

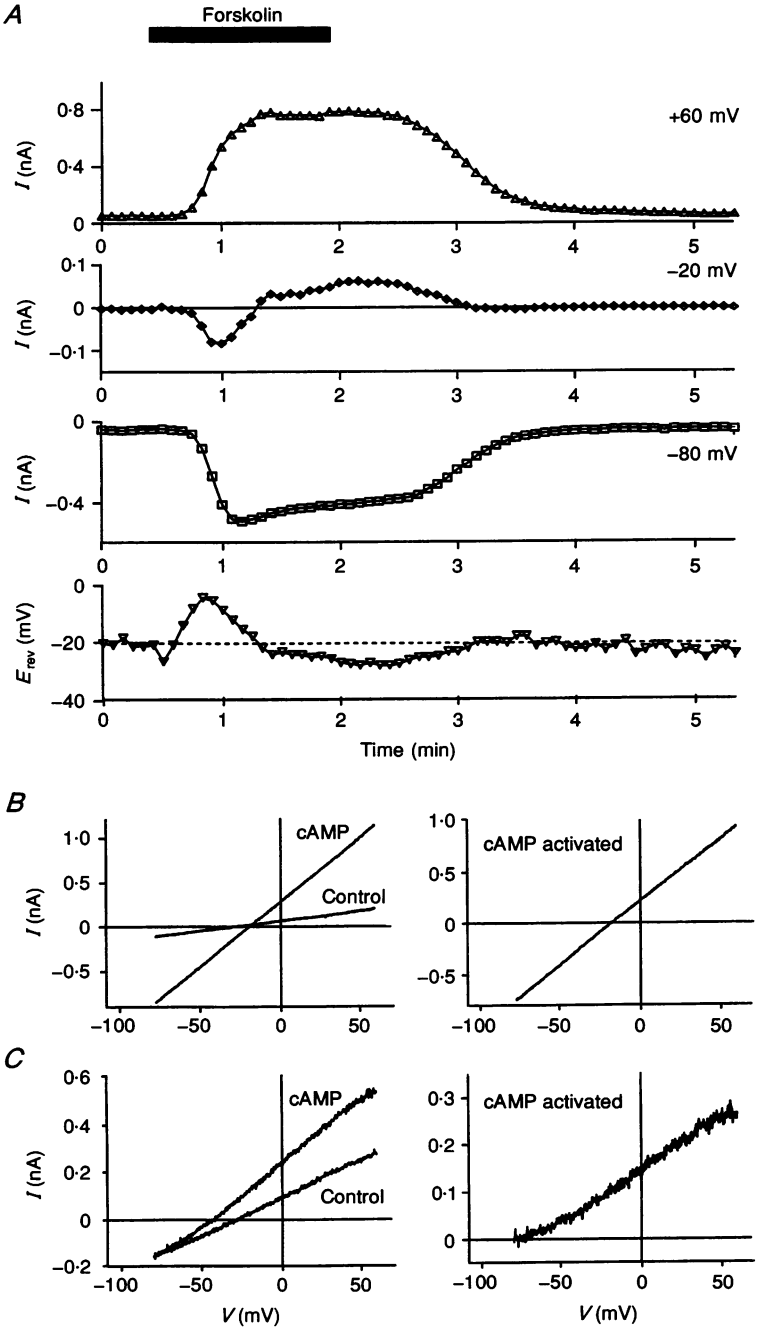

Figure 1. Effects of forskolin (10 μM)
A, currents at +60, −20, and −80 mV, and reversal potential, E_{rev}, recorded during ramps. Forskolin (10 μM) was applied as indicated by the bar. *B* and *C*, *I–V* curves recorded during depolarizing ramps, under control conditions and when cAMP was increased (left panels) in two different cells. The right panels represent the cAMP-activated current *versus* voltage. E_{rev}, −18·1 (*B*) and −85·5 mV (*C*).

with the current as ordinate and the voltage as abscissa. In some experiments, a step protocol was also applied: voltage steps from −60 mV to various potentials between −100 and +60 mV were imposed for 500 ms every 2 s and the isochronal currents at 15 and 450 ms (initial and late currents, respectively) were plotted *versus* potential. Current and voltage data were also recorded on digital audio tapes (DTR1202, Biologic). The leak current was not corrected.

Data are presented as means ± S.E.M.

RESULTS

cAMP activates both Cl^- and K^+ currents

As previously reported by others (Worrell *et al.* 1989; Cliff & Frizzell, 1990; Anderson & Welsh, 1991, Chan *et al.* 1992), the whole-cell current of T84 cells measured in control conditions typically remained stable and had a low amplitude under conditions that prevented cell swelling

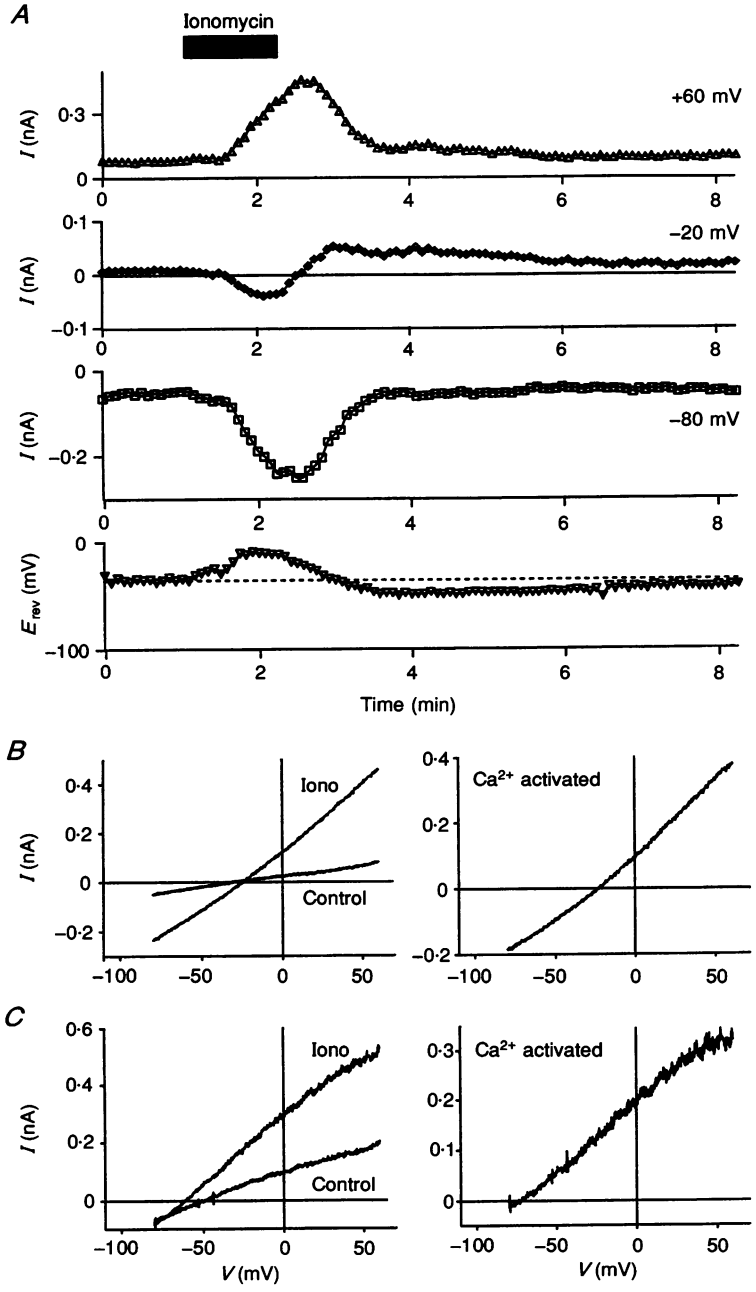

Figure 2. Effects of ionomycin (1 μM)

A, currents recorded at +60, −20, and −80 mV, and E_{rev} during ramps. Ionomycin was applied as indicated by the bar. *B* and *C*, *I–V* curves recorded during depolarizing ramps, under control conditions and when $[Ca^{2+}]_i$ was increased (left panels) in two different cells. The right panels represent the Ca^{2+}-activated current *versus* voltage. E_{rev}, −24·1 (*B*) and −73·8 mV (*C*).

(see Methods and also Worrell *et al.* 1989). In twenty-three different cells, the mean current was $5{\cdot}43 \pm 0{\cdot}81$ pA pF^{-1} at +60 mV and its reversal potential was $-38{\cdot}4 \pm 2{\cdot}5$ mV. In rare instances, bursts of oscillating current activity occurred spontaneously under control conditions (not illustrated). Spontaneously active cells were not kept for further studies.

In T84 cells, cAMP-activated Cl^- channels similar to the cystic fibrosis transmembrane conductance regulator (CFTR). channels affected in cystic fibrosis have previously been reported (Tabcharani *et al.* 1990). We used forskolin, an agonist of adenylyl cyclase, to increase intracellular cAMP. In the presence of the agonist (10 μM), a maximum rise in the total current at +60 mV from $3{\cdot}81 \pm 0{\cdot}61$ up to $20{\cdot}79 \pm 5{\cdot}08$ pA pF^{-1} was observed in eighteen responding cells of twenty-eight (64%). In thirteen of eighteen cells, the current activated by forskolin had a biphasic time course. Figure 1*A* depicts in such a cell the variations in the current measured at +60, −20 and −80 mV and the reversal potential, E_{rev}, for the whole-cell current during voltage ramps applied every 5 s. Under our experimental conditions, the current at +60 mV represents a sum of the activity of Cl^- currents, of the non-specific cationic current (Cliff & Frizzell, 1990; Devor & Duffey, 1992) and of K^+ currents. The current at −80 mV, when inward, presumably represents the activity of Cl^- currents and of the non-specific cationic current. The current at −20 mV represents the activity of K^+ currents (in the outward direction) and of the non-specific cationic current (in the inward direction). During the initial effects of forskolin, the reversal potential was transiently shifted towards more positive potentials and the net current at −20 mV was inward. During the secondary phase, the reversal potential was shifted

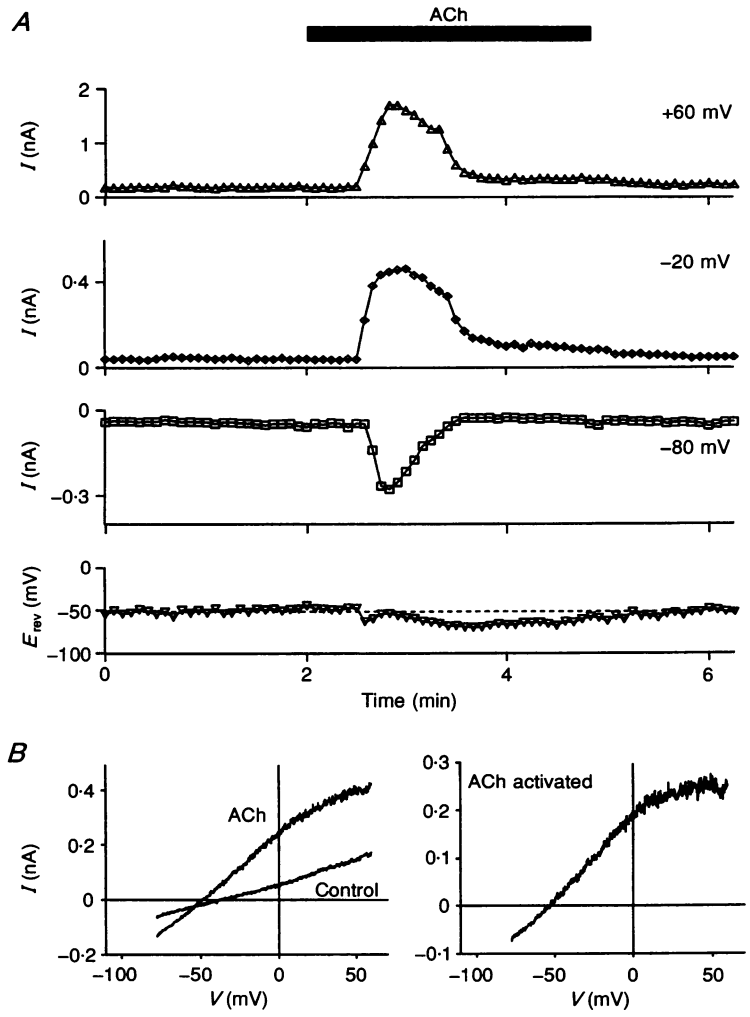

Figure 3. Effects of acetylcholine (1 μM)
A, the currents at +60, −20, and −80 mV, and E_{rev} recorded during ramps. Acetylcholine was applied as indicated by the bar. *B*, *I–V* curves recorded in a different cell during depolarizing ramps, under control conditions and in the presence of ACh (left panel). The right panel represents the ACh-activated current *versus* voltage. E_{rev}, −53·1 mV.

towards negative potentials and the net current at −20 mV was outward. In Fig. 1*B*, the left panel shows superimposed *I–V* curves of the current in control and during the initial phase whereas the right panel shows the initial cAMP-activated current obtained by digitally subtracting the current in control conditions from that recorded in the presence of forskolin. The initial cAMP-activated current had a mean reversal potential of −18·2 ± 1·2 mV. In five of eighteen cells, the current activated by forskolin evolved monophasically. On two occasions, as illustrated in Fig. 1*C*, the reversal potential was directly shifted towards more negative values (reversal potential of the cAMP-activated current: −86·5 mV; i.e. close to E_K). In three other cells, the reversal potential was shifted monophasically towards more positive values (not illustrated).

We interpret these results as suggesting that increased cAMP activated both Cl^- and K^+ currents in T84 cells. In cells showing equilibrated activation of Cl^- and K^+ currents, the rise in the K^+ current was slow and delayed with respect to the rise in the Cl^- current. In addition to Cl^- and K^+ currents, forskolin could also have activated the non-specific cationic current, which was probably responsible for the transient net inward current at −20 mV.

Intracellular Ca^{2+} activates both Cl^- and K^+ currents

In T84 cells, a Cl^- conductance activated by intracellular Ca^{2+} has been reported (Cliff & Frizzell, 1990; Anderson & Welsh, 1991; Worrell & Frizzell, 1991; Chan *et al.* 1992; Devor & Duffey, 1992). We used ionomycin, a Ca^{2+}-

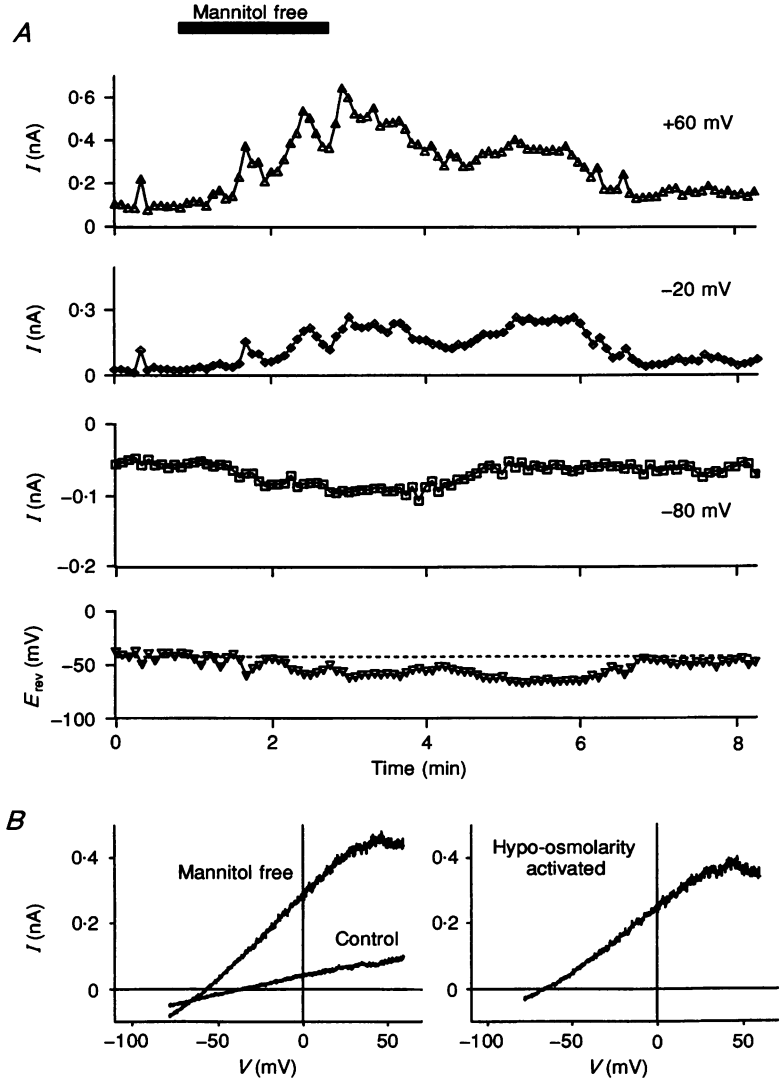

Figure 4. Effects of osmolarity changes
A, the currents at +60 and −80 mV, and E_{rev} recorded during ramps. Mannitol was omitted from the external medium during the time indicated by the horizontal bar. *B*, *I–V* curves recorded during depolarizing ramps, under control conditions and in the absence of mannitol (left panel; same cell as in *A*). The right panel represents the hypo-osmolarity-activated current *versus* voltage. E_{rev}, −65·7 mV.

ionophore, to increase intracellular Ca^{2+} ($[Ca^{2+}]_i$) and thereby to activate Ca^{2+}-dependent currents. In this set of experiments, Ca^{2+} was omitted from the external medium. Ca^{2+} activity (about 8 μM) due to contamination was reduced to 2–3 μM by addition of EGTA. A computer program designed by G. L. Smith (University of Glasgow, UK) was used to estimate the EGTA concentration (5 μM) needed to reach the chosen Ca^{2+} activity. Addition of the ionophore induced an increase in the current recorded at +60 mV from 7·79 ± 1·57 to 57·50 ± 12·10 pA pF^{-1} ($n = 6$). In five cells, the increase in the total current produced by ionomycin and the reversal potential evolved with a biphasic time course (Fig. 2*A*) similar to that observed with forskolin. In Fig. 2*B* the left panel shows the *I–V* curves of the total current in control and during the initial phase, whereas the right panel shows the initial Ca^{2+}-activated current. In the cell illustrated in Fig. 2*C*, the reversal potential was shifted monophasically towards E_K.

Increase in $[Ca^{2+}]_i$ was also attained through the activation of muscarinic receptors with acetylcholine (ACh; 1 μM). ACh increased the maximum current at +60 mV from 6·36 up to 34·13 pA pF^{-1} ($n = 4$). By contrast with the pattern observed with forskolin or ionomycin, the net current at −20 mV was never observed as inward

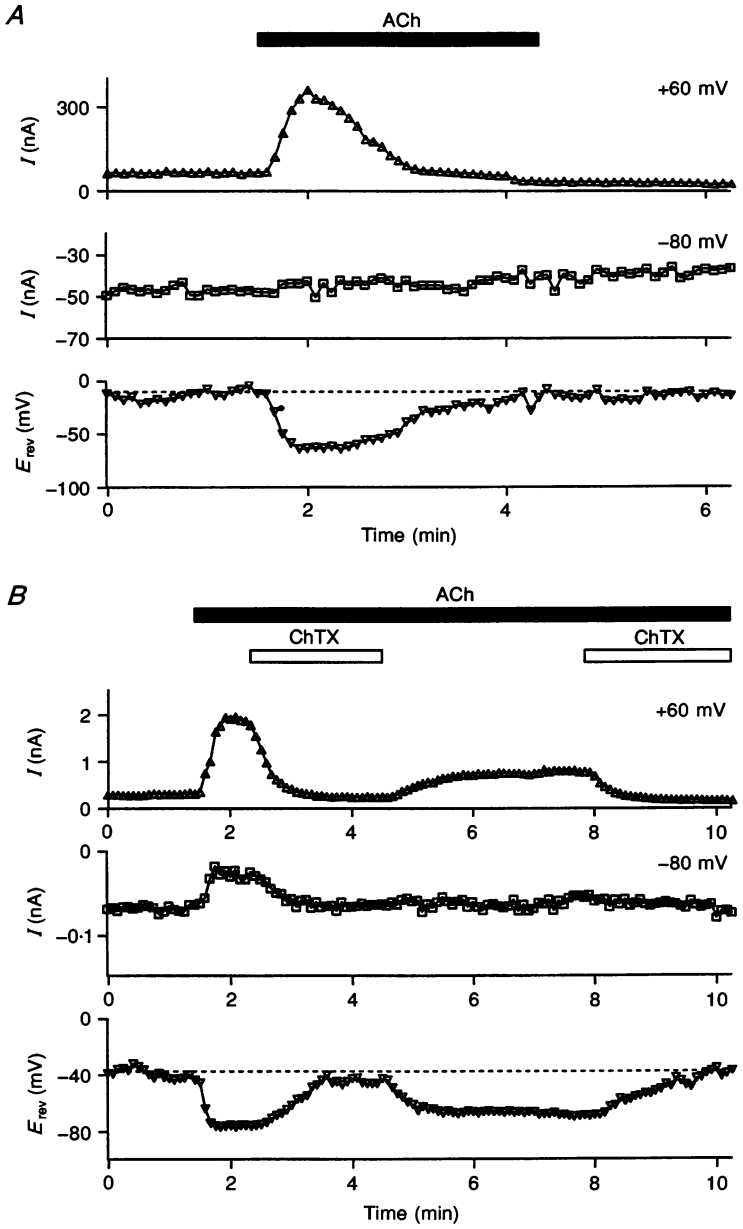

Figure 5. Effects of acetylcholine (1 μM) and charybdotoxin (ChTX; 10 nM) in Cl^--free conditions

A, the currents recorded at +60 and −80 mV, and E_{rev} recorded during ramps. *B*, the effects of ChTX on the current response to ACh (different cell from *A*). ACh and ChTX were applied as indicated by the bars.

in the presence of acetylcholine (Fig. 3*A*). Figure 3*B* shows the current activated by ACh. This current exhibited an inward rectification in the positive potential range and a reversal potential more negative than E_{Cl}. Thus, as previously reported by Devor & Duffey (1992), stimulation of muscarinic receptors led to the immediate activation of K^+ currents. Doses as low as 10 nM ACh were able to activate Ca^{2+}-dependent currents in our cells (not illustrated).

Hypo-osmolarity activates both Cl^- and K^+ currents

Activation of Cl^- currents secondary to reduced external osmolarity has previously been reported in T84 cells (Worrell *et al.* 1989). External hypo-osmolarity was induced by omitting mannitol from the perfused solution. As depicted in Fig. 4*A*, the outward current recorded at +60 mV increased markedly (from $6{\cdot}87 \pm 2{\cdot}12$ to $40{\cdot}79 \pm 15{\cdot}07$ pA pF^{-1}; $n = 5$), as did the inward current at −80 mV, albeit more slightly (from $-2{\cdot}32 \pm 0{\cdot}32$ to $-8{\cdot}91 \pm 4{\cdot}55$ pA pF^{-1}). The *I–V* curve of the current recorded during the hypo-osmotic shock (Fig. 4*B*), showed that the reversal potential was shifted towards E_K (from $-46{\cdot}2 \pm 5{\cdot}0$ to $-53{\cdot}2 \pm 4{\cdot}2$ mV) and that an inwardly rectifying current was activated. The effects of hypo-osmolarity were reversible.

Ca^{2+}-activated K^+ currents

When gluconate was substituted for Cl^-, the mean current at +60 mV was $5{\cdot}19 \pm 0{\cdot}49$ pA pF^{-1} and the reversal potential was $-39{\cdot}5 \pm 1{\cdot}9$ mV ($n = 49$). Under Cl^--free conditions, ACh (1 μM) produced a marked increase in the current at +60 mV from $4{\cdot}24 \pm 0{\cdot}77$ to $17{\cdot}54 \pm 3{\cdot}08$ pA pF^{-1} ($n = 19$) and a shift in the reversal potential from $-37{\cdot}9 \pm 2{\cdot}7$ to $-70{\cdot}5 \pm 2{\cdot}5$ mV. The current activated by ACh had a reversal potential of $-89{\cdot}5 \pm 0{\cdot}2$ mV ($n = 19$),

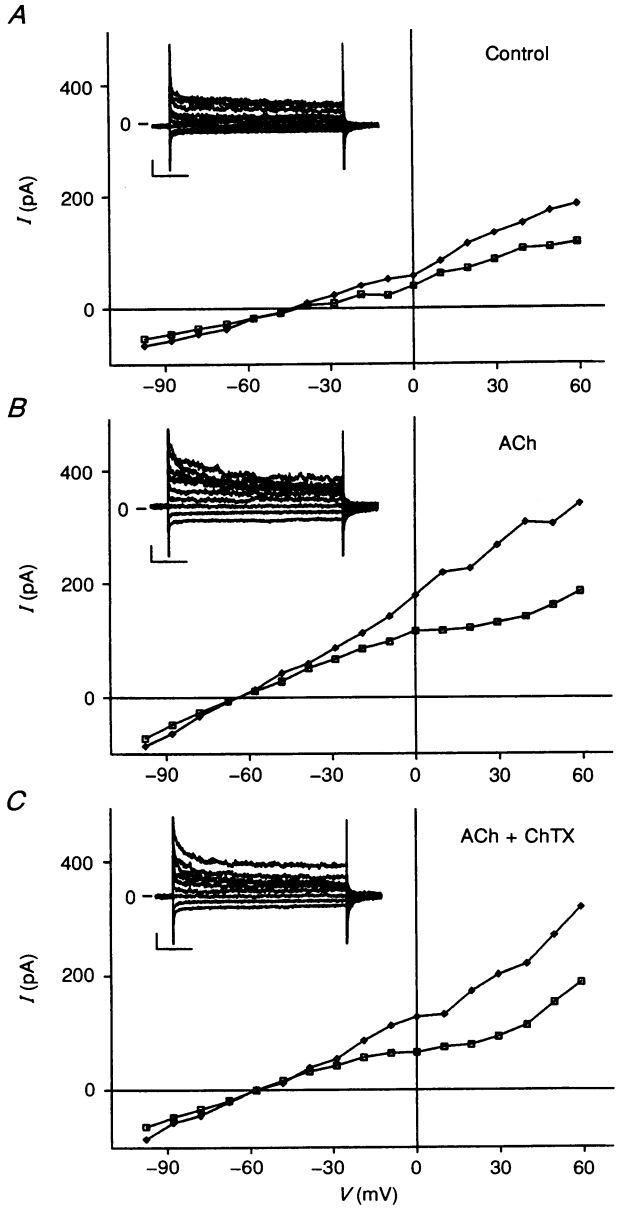

Figure 6. Effects of acetylcholine (1 μM) and charybdotoxin (10 nM) in Cl^--free conditions – the different ACh-activated K^+ currents
A, *I–V* curves recorded at 15 (i_{init}, ◇) and 450 ms (i_{late}, □) during 500 ms voltage steps in control conditions. The insets show superimposed current recordings during voltage steps in 20 mV increments from −60 mV to variable potentials between −100 and +60 mV (horizontal scale bar, 100 ms; vertical scale bar, 0·1 nA). *B*, same as *A* in the presence of ACh. *C*, same as *A* and *B* in the presence of ACh (1 μM) plus ChTX (10 nM).

i.e. close to the equilibrium potential for K^+ ions, under our experimental conditions. Figure 5 illustrates the kinetics of the effects of ACh. In the experiment shown in Fig. 5*A*, ACh only transiently activated K^+ currents. In other instances, as in Fig. 5*B*, ACh produced a transient peak followed by a more sustained response. We used charybdotoxin (ChTX, Latoxan, Rosans, France), a toxin isolated from the venom of the scorpion *Leiurus quinquestriatus hebraeus*, which acts as a specific blocker of Ca^{2+}-dependent K^+ current (MacKinnon & Miller, 1988), to characterize better the current activated by ACh. ChTX 10 nM produced a remarkable inhibition of the ACh-induced outward current at +60 mV (Fig. 5*B*). However, because the response to ACh was largely transient (see Fig. 5*A*), the potency of ChTX to block ACh effects was difficult to assess precisely. Thus, the effects of ChTX were evaluated when the difference between the current in the presence of the toxin and the current recorded after its wash out is considered (Fig. 5*B*).

When a voltage step protocol was used, both time-dependent and -independent currents were recorded in the presence of ACh. In Fig. 6, *I–V* curves of the initial (15 ms) and late (450 ms) currents during voltage steps in control (Fig. 6*A*), in the presence of 1 μM ACh (Fig. 6*B*) and in the presence of 1 μM ACh plus 10 nM ChTX (Fig. 6*C*) are shown. Figure 6*A* shows that under control conditions the outward current was made up of a time-independent component and a time-dependent component which slowly declined during the voltage steps and which were responsible for the difference between the initial and late *I–V* curves. ACh consistently increased the time-dependent component, and also activated a time-independent current which peaked at approximately 0 mV. At 10 nM, ChTX suppressed most of the time-independent component activated by ACh but only slightly reduced the time-dependent component.

Figure 7*A* (upper panel) presents the *I–V* curves of the ACh-activated current determined by digital subtraction 15 (i_{init}) and 450 ms (i_{late}) after the beginning of the pulse. The *I–V* curve of the time-dependent component (i.e. $i_{init} - i_{late}$) shows that this component activated at potentials more positive than −40 mV. The lower panel of Fig. 7*A* represents the *I–V* relation of the ACh-induced late current that was blocked by ChTX in the same cell. Figure 7*B* illustrates results obtained with a voltage ramp protocol. When this protocol was used, ACh induced an

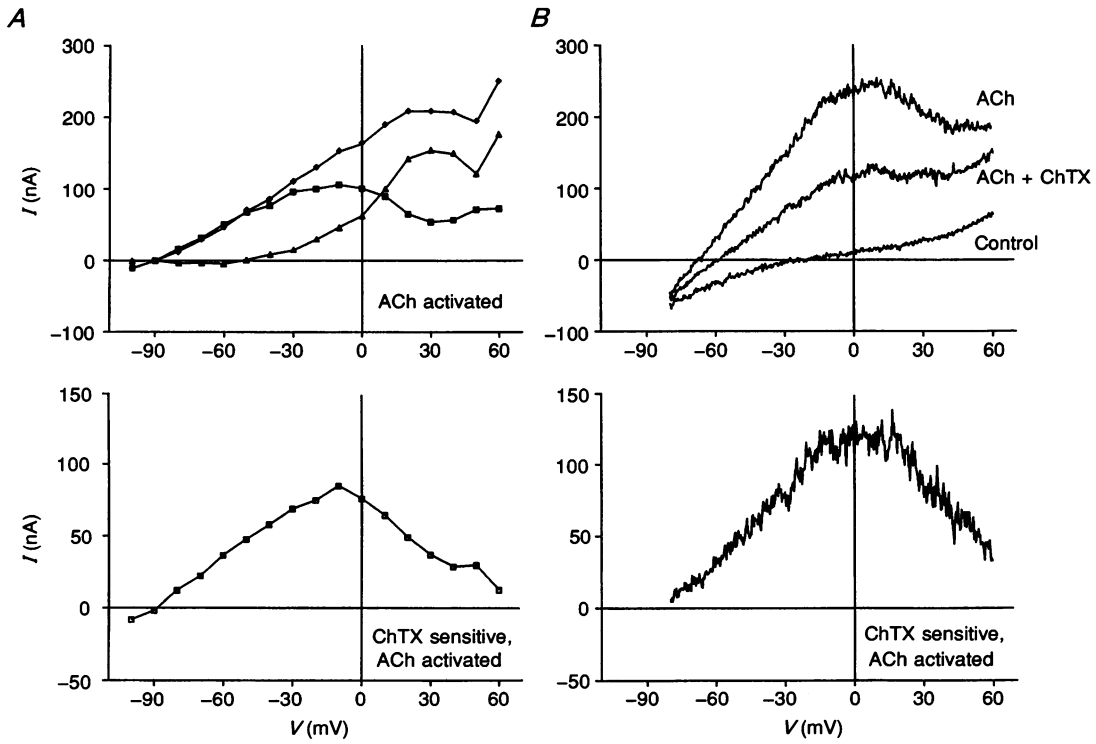

Figure 7. Effects of acetylcholine (1 μM) and charybdotoxin (10 nM) in Cl^--free conditions – the ACh-activated, ChTX-sensitive K^+ current

A, upper panel: *I–V* curves of the initial (◇), late (□) and initial − late (△) ACh-activated currents recorded with a voltage step protocol. The current activated by ACh was obtained by digitally subtracting the current in control conditions from that recorded in the presence of the agonist. Lower panel: *I–V* relation of the ACh-activated late current sensitive to ChTX (same cell as upper panel). *B*, upper panel: *I–V* curves recorded during depolarizing ramps, under control conditions, in the presence of ACh, and in the presence of ACh plus ChTX. Lower panel: *I–V* curve of the ChTX-sensitive ACh-activated current (same cell as upper panel).

inwardly rectifying current (Fig. 7*B*, upper panel). The *I–V* curve of the ACh-induced ChTX-sensitive current recorded either with a ramp clamp protocol (Fig. 7*A*) or with a voltage step protocol (Fig. 7*B*) strongly rectified at positive potentials and had a bell-shaped appearance. All together, our results show that elevated intracellular Ca^{2+} activates two types of K^+ currents in T84 cells: (i) a time-independent ChTX-sensitive K^+ current that strongly rectifies in the positive potential range, and (ii) a time-dependent current that is activated at potentials more positive than −40 mV.

The cAMP-activated K^+ currents

The same experimental protocol was followed to explore the cAMP-activated K^+ current in T84 epithelial cells. When a cAMP 'activator cocktail' (containing forskolin (10 μM); cpt–cAMP, a permeant form of cAMP (400 μM); and IBMX, an inhibitor of the phosphodiesterase (100 μM))

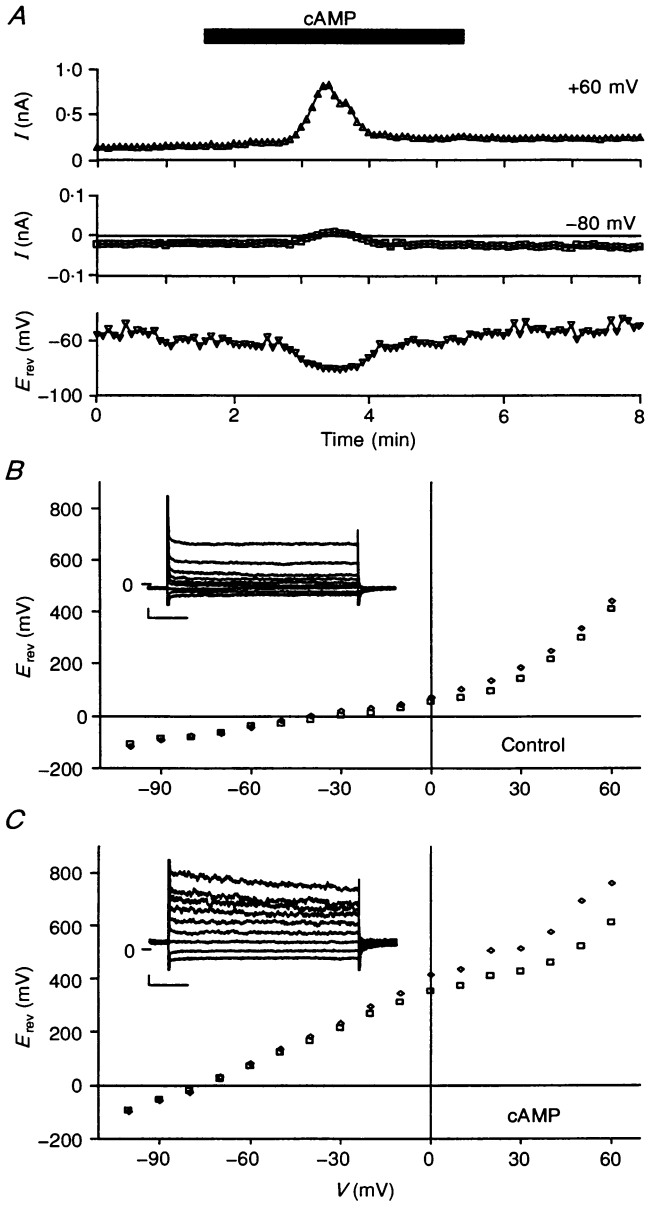

Figure 8. Effects of the cAMP 'activator cocktail' (10 μM forskolin; 100 μM IBMX; 400 μM cpt–cAMP) in Cl^--free conditions

A, the currents recorded at +60 and −80 mV, and E_{rev} recorded during ramps. The activator cocktail (cAMP) was applied as indicated by the horizontal bar. *B* and *C*, initial (◇) and late (□) *I–V* curves recorded with a 500 ms voltage step protocol in control conditions (*B*) and in the presence of the activator cocktail (*C*). The insets show current traces recorded during voltage steps from −60 mV to variable potentials between −100 and +60 mV (horizontal scale bar, 100 ms; vertical scale bar, 0·1 nA).

was added, a mean maximum increase in the current measured at +60 mV occurred from 5·55 ± 0·68 to 18·66 ± 0·36 pA pF^{-1} ($n = 28$). Concomitantly, the reversal potential shifted from −40·5 ± 2·6 to −71·4 ± 1·8 mV. The reversal potential of the cAMP-activated current was −86·8 ± 0·1 mV. Typical results recorded during both voltage ramp and step protocols are illustrated in Fig. 8. As with ACh, the increase in the total current produced by cAMP was mostly transient. Comparison of the initial and late current I–V curves in normal and high $[cAMP]_i$ (Fig. 8*B* and *C*), shows that two types of current were activated: a time-independent inwardly rectifying current and also a time-dependent current, slowly inactivating during the voltage pulse. The I–V curves of the cAMP-activated currents were drawn (Fig. 9*A*). As already observed with ACh, the time-dependent current was not activated at lower potentials and the time-independent current was inwardly rectified. The currents elicited by voltage ramps in another cell and the I–V curve of the ChTX-sensitive cAMP-activated current are depicted in Fig. 9*B* and *C*. Again, the current recorded in high $[cAMP]_i$ showed an inward rectification and was decreased in amplitude by ChTX. From this set of experiments, we concluded that increasing $[cAMP]_i$ induces the activation of two types of K^+ currents: (i) a time-independent ChTX-sensitive current showing strong inward rectification, and (ii) a time-dependent current activated during depolarization. Both currents were comparable with those activated

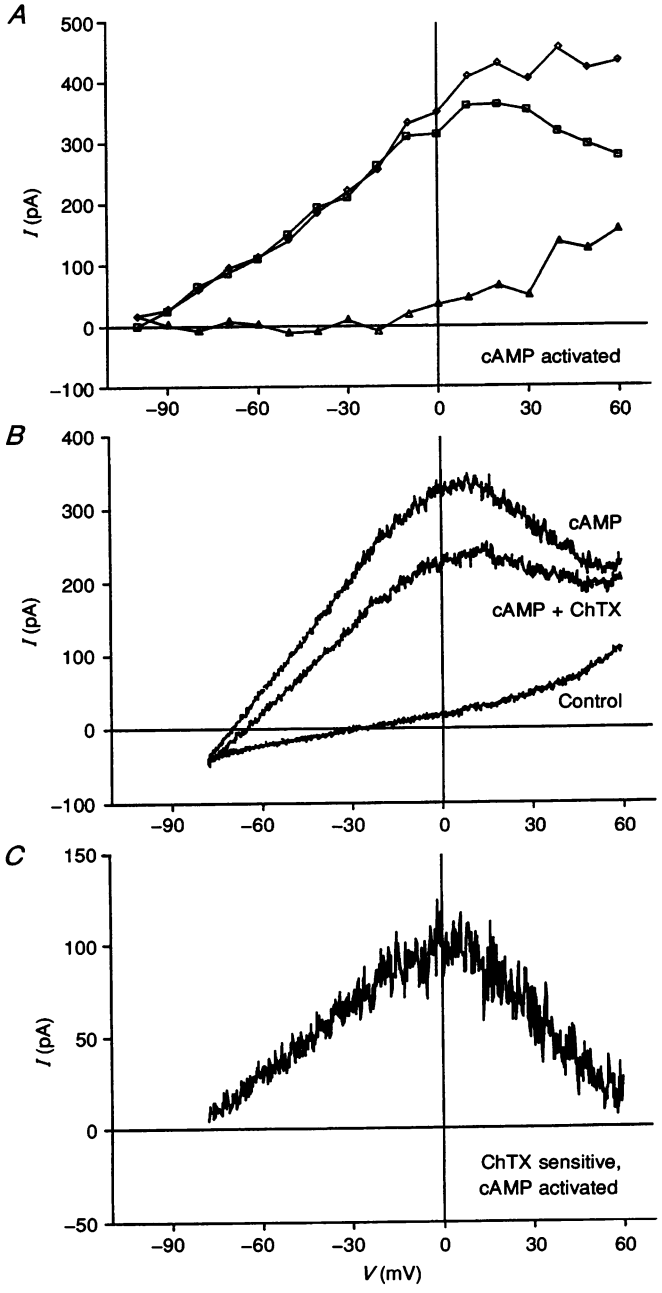

Figure 9. Effects of the cAMP 'activator cocktail' in Cl^--free conditions – the different cAMP-activated K^+ currents
A, I–V curves of the initial (◇), late (□) and initial − late (△) cAMP-activated currents recorded with a voltage step protocol. *B*, I–V curves recorded during depolarizing ramps, under control conditions, in the presence of the activator cocktail and in the presence of the activator cocktail + ChTX (10 nM). *C*, the I–V curve of the cAMP-activated current (same cell as shown in *B*) sensitive to ChTX.

by ACh although the time-dependent component was much smaller in the presence of increased cAMP than in the presence of ACh.

DISCUSSION

Concomitant activation of Cl^- and K^+ currents

Our results show that the increase in Cl^- conductance resulting either from the activation of the cAMP or the Ca^{2+} pathways is *always* simultaneous with an increased K^+ conductance although, depending on the cell, either the K^+ or the Cl^- conductance predominates over the other. The fact that secretagogues increase K^+ conductance is crucial to recycling K^+ at the basolateral membrane and to maintaining a favourable electrical gradient for Cl^- extrusion at the apical membrane. The use of nystatin allowed us to perform reliable whole-cell recordings under conditions where cell wash-out was prevented as discussed by Horn & Marty (1988). Since stimulatory effects of receptor agonists on Cl^--secreting epithelia are transduced by second messengers, the preservation of the intracellular medium permitted the description of different ionic current species under more physiological conditions than those provided by the 'conventional' whole-cell configuration. For example, using the disrupted-patch whole-cell configuration in T84 cells, Cliff & Frizzell (1990) observed with forskolin a sustained increase in Cl^- currents but no K^+ current activation. These authors also observed a transient activation of K^+ currents and a sustained activation of Cl^- currents in response to elevated $[Ca^{2+}]_i$. Using the same configuration, Devor, Simasko & Duffey (1990) found that carbachol induced an oscillating Ca^{2+}-activated K^+ conductance but no increase in Cl^- current. We believe that the discrepancies between these studies and ours are due to artifacts arising from wash-out of some intracellular components through the disrupted patch. Indeed, Devor & Duffey (1992) recently reinvestigated the effects of carbachol in T84 cells by making use of the nystatin technique. In contrast with their previous study, they found a co-ordinated activation by carbachol of both K^+ and Cl^- currents. Our findings are in agreement with previous experimental results obtained in intact cells. In canine tracheal epithelium (Halm & Frizzell, 1990), adrenaline produces a rise in apical conductance (presumably caused by a rise in Cl^- conductance) and also a rise in basolateral conductance (presumably caused by a rise in K^+ conductance). In T84 monolayers, the vasoactive intestinal peptide (VIP, an agent that acts by increasing the level of cAMP), the Ca^{2+} ionophore A23187, and carbachol induce a two- to threefold increase in $^{86}Rb^+$ efflux across the basolateral membrane (Mandel, McRoberts, Beuerlein, Forster & Dharmsathaphorn, 1986*b*; Dharmsathaphorn & Pandol, 1986). Furthermore, serosal application of Ba^{2+} (5 mM), inhibits Cl^- secretion induced by VIP, prostaglandin E_1, or A23187 (Weymer *et al.* 1985; Mandel *et al.* 1986*b*). Similarly, in canine airway epithelia, ChTX inhibits the chloride secretion produced by A23187 (McCann & Welsh, 1990). Finally, depolarization of the cell membrane secondary to increased extracellular K^+, markedly decreases the ionomycin- and forskolin-induced Cl^- efflux (Venglarik, Bridges & Frizzell, 1990).

In our cells, concomittant activation of Cl^- and K^+ conductance was also observed under the influence of hypo-osmotic shock. Under these circumstances, which mechanism activates K^+ channels? A likely explanation is that intracellular Ca^{2+} also plays a central role. Increased $[Ca^{2+}]_i$ during hypo-osmotic stress has been reported repetitively in epithelial cells (Hazama & Okada, 1988; Wong, DeBell & Chase, 1990; Nitschke, Leipziger & Greger, 1993) including T84 cells (McEwan, Brown, Hirst & Simmons, 1992) and may result from both Ca^{2+} release from intracellular stores (Nitschke, Leipziger & Greger, 1993) and the influx of Ca^{2+} via stretch-activated non-specific cation channels (Bear, 1990).

Two types of K^+ currents in the T84 cell line

We found that two different types of outward current were activated by agonists in the absence of permeant anions: (i) a time-independent inwardly rectifying K^+ current, sensitive to ChTX, and (ii) a time-dependent outward current, insensitive to ChTX, activated when the cell was depolarized to potentials more positive than −40 mV. With the voltage ramp protocol we used, the time-independent component predominated. Although the ionic nature of the time-dependent current cannot be definitely established from our data, it is probably a K^+ current. A slowly relaxing outward current identified as a K^+ current has previously been reported in T84 cells (see Fig. 5 of Cliff & Frizzell, 1990). In addition to Cl^- and K^+ currents, a non-specific cationic current has been reported in the T84 epithelial cell line (Cliff & Frizzell, 1990; Devor & Duffey, 1992). In human nasal epithelial cells, non-specific cationic channels are equally permeable to K^+ and Na^+, poorly permeable to Ca^{2+} and impermeable to anions (Jorissen, Vereeke, Carmeliet, Van den Berghe & Cassiman, 1990). Furthermore, they are activated by intracellular Ca^{2+} and their open probability is increased by depolarizations. In our experimental conditions, the reversal potential of the cations was approximately 0 mV. Therefore, such non-specific cationic channels cannot underlie an outward current at negative potentials as seen here.

Activation of the same K^+ channels by agonists using different second messengers is puzzling. The fact that K^+ currents were activated in T84 cells by a Ca^{2+} ionophore strongly supports the interpretation that the responsible channels were Ca^{2+}-activated channels. This does not

mean that Ca^{2+} is the only modulator of basolateral K^+ channels. In fact, activation of apical Cl^- channels in T84 cells submitted to increased $[Ca^{2+}]_i$ is not direct but rather involves a calcium–calmodulin protein kinase (Worell & Frizzell, 1991). The same kinase may also regulate basolateral K^+ channels. Most recently, Kachintorn, Vonkovit, Vajanpanich, Dinh, Barett & Dharmsathaphorn (1992) proposed that Ca^{2+}-dependent secretagogues exert dual effects on chloride secretion: (i) an initial stimulatory effect related to increased $[Ca^{2+}]_i$, and (ii) a delayed inhibitory effect related to the activation of protein kinase C. Inhibition of Cl^- secretion by protein kinase C is partly supported by a protein kinase C-dependent block of basolateral K^+ channels (Reenstra, 1993). Thus, the modulation of basolateral K^+ channel by acetylcholine is not necessarily straightforward, i.e. Ca^{2+}-mediated, but may also involve calcium–calmodulin protein kinase and/or protein kinase C.

In airway epithelium, cpt–cAMP, a permeable analogue of cAMP, and the β-adrenergic agonist isoprenaline induce a transient increase in $[Ca^{2+}]_i$ which is directly measured using the Ca^{2+}-sensitive fluorescent probe fura-2 (McCann, Bhalla & Welsh, 1989). Similarly, in Madin–Darby canine kidney cells β-adrenergic agonists and cAMP analogues increase $[Ca^{2+}]_i$ (Chase & Wong, 1988), though the intracellular source of the Ca^{2+} released by cAMP is not yet known. Conversely, increased intracellular Ca^{2+} may result in stimulation of the arachidonate metabolism and subsequent prostaglandin production and thereby an increase in cellular levels of cAMP (McCann, Bhalla & Welsh, 1989). Thus, the two secretagogue pathways are not totally independent but, on the contrary, are possibly interconnected. In T84 cells, agonists that increased $[Ca^{2+}]_i$ produce effects on Rb^+ efflux which are additive to those produced by agonists acting via the cAMP pathway (Dharmsathaphorn & Pandol, 1986). This finding was used as an argument to suggest that two categories of basolateral K^+ channels may be activated in T84, one regulated by Ca^{2+} and the other regulated via protein phosphorylation with protein kinase A (McRoberts *et al.* 1985; Dharmsathaphorn & Pandol, 1986; Mandel *et al.* 1986*b*). Our data oppose this hypothesis since, in our experiments, the same K^+ currents were activated by both pathways. A possible interpretation that would reconcile both findings is to assume that basolateral K^+ channels are regulated not only by $[Ca^{2+}]_i$ but also by protein kinase A. Depending on the secretory agonist, one or the other (or both) regulatory mechanism(s) is (are) used to increase K^+ conductance. Such Ca^{2+}-activated K^+ channels sensitive to cAMP-dependent phosphorylation have been found in cultured kidney cells (Guggino, Suarez-Isla, Guggino & Sacktor, 1985) and in pancreatic duct cells (Gray, Greenwell, Garton & Argent, 1990).

In cystic fibrosis secretory cells, the K^+ permeability of the epithelium is not altered (Welsh & Liedtke, 1986; Kunzelmann *et al.* 1989; Goldstein, Shapiro, Rao & Layden, 1991). It is hypothesized that the activation of K^+ channel activity may be sufficient *per se* to amplify the background Cl^- secretion, whatever the underlying Cl^- channel class and its activation mode. This assumption may have important therapeutic implications in the context of cystic fibrosis. The exact nature of the K^+ channels implicated in chloride secretion thus needs further investigation.

REFERENCES

Anderson, M. P. & Welsh, M. J. (1991). Calcium and cAMP activate different chloride channels in the apical membrane of normal and cystic fibrosis epithelia. *Proceedings of the National Academy of Sciences of the USA* **88**, 6003–6007.

Bear, C. (1990). A nonselective cation channel in rat liver cells is activated by membrane stretch. *American Journal of Physiology* **258**, C421–428.

Chan, H. C., Kaetzel, M. A., Nelson, D. J., Hazarika, P. & Dedman, J. R. (1992). Antibody against a cystic fibrosis transmembrane conductance regulator-derived synthetic peptide inhibits anion currents in human colonic cell line T84. *Journal of Biological Chemistry* **267**, 8411–8416.

Chase, H. S. & Wong M. E. (1988). Isoproterenol and cAMP increase intracellular free Ca in MDCK cells. *American Journal of Physiology* **254**, F374–384.

Cliff, W. H. & Frizzell, R. A. (1990). Separate Cl^- conductances activated by cAMP and Ca^{2+} in Cl^- secreting epithelial cells. *Proceedings of the National Academy of Sciences of the USA* **87**, 4956–4960.

Devor, D. C. & Duffey, M. E. (1992). Carbachol induces K^+, Cl^-, and nonselective cation conductances in T84 cells: a perforated patch-clamp study. *American Journal of Physiology* **263**, C780–787

Devor, D. C., Simasko, S. M. & Duffey, M. E. (1990). Carbachol induces oscillations of membrane potassium conductance in a colonic cell line, T84. *American Journal of Physiology* **258**, C318–326.

Dharmsathaphorn, K., Cohn, J. A. & Beuerlein, G. (1989). Multiple calcium-mediated effector mechanisms regulate chloride secretory responses in T84 cells. *American Journal of Physiology* **256**, C1224–1230.

Dharmsathaphorn, K. & Pandol, S. J. (1986). Mechanism of chloride secretion induced by carbachol in a colonic epithelial cell line. *Journal of Clinical Investigation* **77**, 348–354.

Goldstein, J. L., Shapiro, A. B., Rao, M. C. & Layden, T. J. (1991). In vivo evidence of altered chloride but not potassium secretion in cystic fibrosis rectal mucosa. *Gastroenterology* **101**, 1012–1019.

Gray, M. A., Greenwell, J. R., Garton, A. J. & Argent, B. E. (1990). Regulation of Maxi-K^+ channels on pancreatic duct cells by cyclic AMP-dependent phosphorylation. *Journal of Membrane Biology* **115**, 203–215.

Guggino, S. E., Suarez-Isla, B. A., Guggino, B. & Sacktor, B. (1985). Forskolin and antidiuretic hormone stimulate a Ca^{2+}-activated K^+ channel in cultured kidney cells. *American Journal of Physiology* **249**, F448–455.

Halm, D. R. & Frizzell, R. A. (1990). Intestinal chloride secretion. In *Textbook of Secretory Diarrhea*, ed. Lebenthal, E. & Duffey, M., pp. 47–58. Raven Press Ltd, New York.

Halm, D. R. & Frizzell, R. A. (1992). Anion permeation in an apical membrane chloride channel of a secretory epithelial cell. *Journal of General Physiology* **99**, 339–366.

HAZAMA, A. & OKADA, Y. (1988). Ca^{2+}-sensitivity of volume-regulated K^+ and Cl^- channels in cultured human epithelial cells. *Journal of Physiology* **402**, 687–702.

HORN, R. & MARTY, A. (1988). Muscarinic activation of ionic currents measured by a new whole-cell recording method. *Journal of General Physiology* **92**, 125–159.

JORISSEN, M., VEREEKE, J., CARMELIET, E., VAN DEN BERGHE, H. & CASSIMAN, J. J. (1990). Identification of a voltage- and calcium-dependent non-selective cation channel in cultured adult and fetal human nasal epithelial cells. *Pflügers Archiv* **415**, 617–623.

KACHINTORN, U., VONGKOVIT, P., VAJANAPHANICH, M., DINH, S., BARETT, K. E. & DHARMSATHAPHORN, K. (1992). Dual effects of phorbol ester on calcium-dependent chloride secretion by T84 epithelial cells. *American Journal of Physiology* **262**, C15–22.

KUNZELMANN, K., PAVENSTÄDT, H., BECK, C., ÜNAL, Ö., EMMRICH, P., ARNDT, H. J. & GREGER, R. (1989). Characterization of potassium channels in respiratory cells. I. General properties. *Pflügers Archiv* **414**, 291–296.

LIN, M., NAIRN, A. C. & GUGGINO, S. E. (1992). cGMP-dependent protein kinase regulation of a chloride channel in T84 cells. *American Journal of Physiology* **262**, C1304–1312.

MCCANN, J. D., BHALLA, R. C. & WELSH, M. J. (1989). Release of intracellular calcium by two different second messengers in airway epithelium. *American Journal of Physiology* **257**, L116–124.

MCCANN, J. D. & WELSH, M. J. (1990). Regulation of Cl^- and K^+ channels in airway epithelium. *Annual Review of Physiology* **52**, 115–135.

MCEWAN, G. T. A., BROWN, C. D. A., HIRST, B. H. & SIMMON, S. N. L. (1992). Hypo-osmolar stimulation of transepithelial Cl^- secretion in cultured human T84 intestinal epithelial layers. *Biochimica et Biophysica Acta* **1135**, 180–183.

MACKINNON, R. & MILLER, C. (1988). Mechanism of Charybdotoxin block of the high-conductance, Ca^{2+}-activated K^+ channel. *Journal of General Physiology* **91**, 335–349.

MCROBERTS, J. A., BEUERLEIN, G. & DHARMSATHAPHORN, K. (1985). Cyclic AMP and Ca^{2+}-activated K^+ transport in a human colonic epithelial cell line. *Journal of Biological Chemistry* **260**, 14163–14172.

MANDEL, K. G., DHARMSATHAPHORN, K. & MCROBERTS, J. A. (1986*a*). Characterization of a cyclic AMP-activated Cl^- transport pathway in the apical membrane of a human colonic epithelial cell line. *Journal of Biological Chemistry* **261**, 704–712.

MANDEL, K. G., MCROBERTS, J. A., BEUERLEIN, G., FOSTER, E. S. & DHARMSATHAPHORN, K. (1986*b*). Ba^{2+} inhibition of VIP and A23187-stimulated Cl^- secretion by T84 cell monolayers. *American Journal of Physiology* **250**, C486–494.

NITSCHKE, R., LEIPZIGER, J. & GREGER, R. (1993). Intracellular transients in HT29 cells induced by hypotonic cell swelling. *Pflügers Archiv* **423**, 274–279.

QUINTON, P. M. (1990). Cystic fibrosis: a disease in electrolyte transport. *FASEB Journal* **4**, 2709–2717.

REENSTRA, W. W. (1993). Inhibition of cAMP and Ca-dependent Cl^- secretion by phorbol esters: inhibition of basolateral K^+ channels. *American Journal of Physiology* **264**, C161–168.

SHOROFSKY, S. R., FIELD, M. & FOZZARD, H. A. (1984). Mechanism of chloride secretion in canine trachea: changes in intracellular chloride activity with secretion. *Journal of Membrane Biology* **81**, 1–8.

TABCHARANI, J. A., LOW, W., ELIE, D. & HANRAHAN, J. W. (1990). Low-conductance chloride channel activated by cAMP in the epithelial cell line T84. *FEBS Letters* **270**, 157–164.

VENGLARIK, C. J., BRIDGES, R. J. & FRIZZELL, R. A. (1990). A simple assay for agonist-regulated Cl and K conductances in salt-secreting epithelial cells. *American Journal of Physiology* **259**, C358–364.

WAGNER, J. A., COZENS, A. L., SHULMAN, H., GRUENERT, D. C., STRYER, L. & GARNER, P. (1991). Activation of chloride channels in normal and cystic fibrosis airway epithelial cells by multifunctional calcium/calmodulin-dependent protein kinase. *Nature* **349**, 793–796.

WASSERMAN, S. I., BARRETT, K. E., HUOTT, P. A., BEUERLEIN, G., KAGNOFF, M. & DHARMSATHAPHORN, K. (1988). Immune-related intestinal Cl^- secretion. I. Effects of histamine on the T84 cell line. *American Journal of Physiology* **254**, C53–62.

WELSH, M. J. & LIEDTKE C. M. (1986). Chloride and potassium channels in cystic fibrosis airway epithelia. *Nature* **322**, 467–470.

WEYMER, A., HUOTT, P., LIU, W., MCROBERTS, J. A. & DHARMSATHAPHORN, K. (1985). Chloride secretory mechanism induced by prostaglandin E1 in a colonic epithelial cell line. *Journal of Clinical Investigation* **76**, 1828–1836.

WONG, S. M. E., DEBELL, M. C. & CHASE, H. S. JR (1990). Cell swelling increases intracellular free [Ca] in cultured toad bladder cells. *American Journal of Physiology* **258**, F292–296.

WORRELL, R. T., BUTT, A. G., CLIFF, W. H. & FRIZZELL, R. A. (1989). A volume-sensitive chloride conductance in human colonic cell line T84. *American Journal of Physiology* **256**, C1111–1119.

WORRELL, R. T. & FRIZZELL, R. A. (1991). CaMKII mediates stimulation of chloride conductance by calcium in T84 cells. *American Journal of Physiology* **260**, C877–882.

Acknowledgements

This work was supported by special grants from the Association Française de Lutte contre la Mucoviscidose (AFLM), Air Liquide and the Centre National de la Recherche Scientifique (CNRS). We thank Ms Martens for her kind help in improving the English of the manuscript. The technical assistance of Marie-Laure Rallo is also acknowledged.

Received 28 June 1993; accepted 7 January 1994.